

# Collective motion of Josephson vortices in intrinsic Josephson junctions in $\text{Bi}_2\text{Sr}_2\text{CaCu}_2\text{O}_{8+y}$

G. Hechtfisher, R. Kleiner, K. Schlenga, W. Walkenhorst, and P. Müller  
*Physikalisches Institut III, Universität Erlangen-Nürnberg, D-91058 Erlangen, Germany*

H. L. Johnson

*Commonwealth Scientific and Industrial Research Organization, Division of Applied Physics, Lindfield, Australia 2070*

(Received 20 December 1996)

We report on the experimental observation of moving Josephson vortices in mesa structures patterned on the surface of  $\text{Bi}_2\text{Sr}_2\text{CaCu}_2\text{O}_{8+y}$  single crystals. Mesas form stacks of typically 100 intrinsic Josephson junctions. In magnetic fields parallel to the superconducting copper oxide layers, a flux-flow branch develops on the current-voltage ( $I$ - $V$ ) characteristic. We investigate this branch in magnetic fields  $H$  up to 15 kOe for junctions with lateral dimensions ranging from  $20 \times 20 \mu\text{m}^2$  to  $500 \times 20 \mu\text{m}^2$ . Investigations show that the voltage of the branch scales with  $1/H$ . For mesas of the same height its slope is inversely proportional to the junction area showing that the flux-flow resistance is independent of the particular junction length. Microwave emission is sensitive to the direction of fluxon motion. This shows that the flux-flow branch in the  $I$ - $V$  characteristic is caused by the collective motion of vortices. We compare our data to numerical simulations based on the coupled sine-Gordon equations for strongly coupled, stacked Josephson junctions. We show that the observed branch can be understood as a flux-flow state caused by vortices moving with the lowest collective-mode velocity of the system. The value derived for the Swihart velocity is in good agreement with recent measurements of the  $c$ -axis Josephson plasma frequency. [S0163-1829(97)05421-0]

## I. INTRODUCTION

Long Josephson junctions, i.e., junctions where one dimension is larger than the Josephson penetration depth  $\lambda_J$ , have been investigated intensively for several reasons. They are not only a valuable object for theoretical study of nonlinear dynamics,<sup>1</sup> but have also found application as high-frequency sources (flux-flow oscillators). Magnetic flux penetrates into a long Josephson junction in the form of Josephson vortices (or fluxons), carrying one magnetic-flux quantum each. The dynamics of such a system is described by the sine-Gordon equation.<sup>2</sup> The motion of fluxons is characterized mainly by two regimes, the resonant fluxon-antifluxon motion in zero magnetic field giving rise to zero-field steps (ZFS), and the flux-flow regime in large magnetic fields which leads to the flux-flow steps (FFS) in the current-voltage ( $I$ - $V$ ) characteristic. In the last few years, an interesting extension of this topic was provided by vertical stacks of long Josephson junctions. For stacks of Josephson junctions with superconducting electrodes thinner than the London penetration depth  $\lambda$ , the external field will penetrate the electrodes. The resulting screening currents lead to a mutual coupling between adjacent junctions. This inductive coupling is described by a system of coupled sine-Gordon equations.<sup>3,4</sup> Available systems for experimental study of this model are either stacks in Nb-Al/ $\text{AlO}_x$ -Nb technology<sup>5</sup> or the intrinsic Josephson junctions in layered high- $T_c$  superconductors such as  $\text{Bi}_2\text{Sr}_2\text{CaCu}_2\text{O}_{8+y}$  (BSCCO).<sup>6</sup> The latter are naturally formed by adjacent  $\text{CuO}_2$  double layers and the spacing BiO and SrO layers. Using standard lithography, small mesa structures consisting of typically 100 junctions can be fabricated with well-defined geometry on the surface of BSCCO single crystals.<sup>7,8</sup>

Nb-Al/ $\text{AlO}_x$ -Nb stacks allow tuning of the coupling

strength by varying the layer thicknesses. The thickness of the superconducting layers is of the order of  $\lambda$ . Thus the coupling strength can be varied over a wide range up to the case of nearly independent junctions. In contrast, intrinsic Josephson junctions realize nearly perfectly the asymptotic case of strong coupling. The thickness of the superconducting layers is vanishingly small compared to the London penetration depth. For intrinsic Josephson junctions in BSCCO the spacing between the superconducting layers is 12 Å and their thickness is only about 3 Å. In comparison, the London penetration depth  $\lambda_{ab}$  is about 1700 Å, by two orders of magnitude larger than the thickness of one junction of the stack. Whereas the coupling parameter for Nb stacks can be tuned by varying the layer thicknesses, essential parameters of intrinsic Josephson junctions like critical current density or characteristic frequency can be easily tuned by oxygen doping.<sup>6</sup>

Recent experiments by Lee, Nordman, and Hohenwarter showed the existence of a linear branch in the  $I$ - $V$  characteristic of BSCCO mesa structures under the influence of a low magnetic field.<sup>9</sup> Their results were compared to the theory for Josephson vortex flow in layered structures by Clem and Coffey.<sup>10</sup> This theory is based on the assumption that only one single Josephson vortex is moving in the whole structure. It is known from energy arguments,<sup>11</sup> that Josephson vortices form a triangular lattice in the absence of bias current. As this lattice should be stable at least for low bias currents, our aim was to find a more exact explanation of the displaced linear branch. We demonstrate by microwave emission experiments that the observed behavior is caused by *collective* motion of many Josephson vortices.

## II. BASIC CONCEPTS

The dynamics of a vertical stack of Josephson junctions is described by a system of coupled sine-Gordon

equations.<sup>3,4,11,12</sup> The stack consists of  $N$  identical Josephson junctions with maximum Josephson current density  $j_c$  and normal-state conductance  $\sigma$ . Each electrode has a thickness  $d$ , the barrier thickness of each junction is  $t$ , and the dielectric constant is  $\varepsilon$ . In the following, we use the normalized units of Ref. 4. Time is normalized to  $\Phi_0\sigma/(2\pi j_c t)$ , lengths are given in units of  $b$ , the junction length in  $x$  direction. Current densities are normalized to  $j_c$ . The relation between the second spatial derivative of the gauge-invariant phase differences  $\gamma_n$  and the current in junction  $n$  and its neighboring junctions is

$$\gamma_n'' = \left(\frac{b}{\gamma_j}\right)^2 j_n - \left(\frac{b}{\lambda_k}\right)^2 (j_{n-1} + j_{n+1}), \quad n = 1, \dots, N.$$

The second term on the right-hand side introduces the inductive coupling of adjacent junctions. The characteristic lengths  $\lambda_j$  and  $\lambda_k$  are given by

$$\lambda_j = \sqrt{\frac{\Phi_0}{2\pi\mu_0 j_c (t_{\text{eff}} + 2\lambda^2/d_{\text{eff}})}}, \quad \lambda_k = \sqrt{\frac{\Phi_0 d_{\text{eff}}}{2\pi\mu_0 \lambda^2 j_c}}$$

with the effective values  $d_{\text{eff}} = \lambda \sinh(d/\lambda)$  and  $t_{\text{eff}} = t + 2\lambda \tanh[d/(2\lambda)]$ . Boundary conditions are  $j_0 = j_{N+1} = j_{\text{ext}}$ . We introduce a coupling matrix  $M$  with diagonal elements  $M_{i,i} = (b/\lambda_j)^2$ , and nondiagonal elements  $M_{i,i+1} = M_{i,i-1} = -(b/\lambda_k)^2$ . Other elements of  $M$  are zero. Treating  $\boldsymbol{\gamma} = (\gamma_1, \dots, \gamma_n)$  and  $\mathbf{j} = (j_1, \dots, j_n)$  as vectors, the equations including the boundary conditions may be written as

$$\boldsymbol{\gamma}'' = M\mathbf{j} - \left(\frac{b}{\lambda_k}\right)^2 (1, 0, \dots, 0, 1)j_{\text{ext}}.$$

According to the definition of  $M$ , this is equal to

$$\boldsymbol{\gamma}'' = M(\mathbf{j} - \mathbf{1}j_{\text{ext}}) + \mathbf{1}\left(\frac{b}{\lambda_m}\right)^2 j_{\text{ext}},$$

where  $\mathbf{1} = (1, \dots, 1)$ . The magnetic screening length  $\lambda_m$  is defined as

$$\frac{1}{\lambda_m^2} = \frac{1}{\lambda_j^2} - \frac{2}{\lambda_k^2}.$$

The current in each junction is given as the sum of displacement, resistive, and Josephson currents. Thus the whole system of coupled sine-Gordon equations including the boundary conditions may be written in the compact form

$$\boldsymbol{\gamma}'' - \mathbf{1}\left(\frac{b}{\lambda_m}\right)^2 j_{\text{ext}} = M(\beta_c \ddot{\boldsymbol{\gamma}} + \dot{\boldsymbol{\gamma}} + \sin \boldsymbol{\gamma} - \mathbf{1}j_{\text{ext}}), \quad (1)$$

where  $\beta_c = 2\pi\varepsilon\varepsilon_0 j_c t / \sigma^2 \Phi_0$  is the McCumber parameter. For intrinsic Josephson junctions in BSCCO we have typical parameters  $d = 3 \text{ \AA}$ ,  $t = 12 \text{ \AA}$ ,  $\lambda = 1500 \text{ \AA}$ , and  $j_c = 150 \text{ A/cm}^2$  and get  $\lambda_j = 1.1 \text{ \mu m}$  and  $\lambda_k = 1.5 \text{ \mu m}$ . The dimensionless coupling parameter  $s = (\lambda_j/\lambda_k)^2$  expressing the ratio of the nondiagonal to the diagonal elements of  $M$  differs in this case by only  $4 \times 10^{-6}$  from its asymptotic value 0.5. This means that intrinsic Josephson junctions are a perfect realization of strong coupling, as the electrode thickness is much smaller than the London penetration depth. The length  $2\lambda_j$  is the diameter of a Josephson vortex in the static

case. Thus an intrinsic Josephson junction will allow the penetration of vortices in the presence of an external field, when its length exceeds the value of about  $2.2 \text{ \mu m}$ . This condition is fulfilled for all samples used in this work.

Under the influence of a bias current, a Lorentz force is exerted on the Josephson vortices and gives rise to flux flow. In the case of a single long Josephson junction, the maximum velocity of a vortex is given by the Swihart velocity. The Swihart velocity is the phase velocity of small amplitude electromagnetic modes in the long Josephson junction. Further investigation<sup>5,12</sup> of Eq. (1) showed that the stack of  $N$  Josephson junctions has  $N$  different electromagnetic modes. In contrast to the single Swihart velocity of a single junction, in the stack  $N$  different mode velocities exist. They are given by

$$c_n = \omega_{\text{pl}} \lambda_j \frac{1}{\sqrt{1 - 2s \cos[\pi n/(N+1)]}}, \quad n = 1, 2, \dots, N, \quad (2)$$

where  $\omega_{\text{pl}} = [(2\pi j_c t)/(\Phi_0 \varepsilon \varepsilon_0)]^{1/2}$  is the Josephson plasma frequency. Note that with increasing  $n$ , the mode velocity  $c_n$  decreases. The lowest mode velocity corresponds to  $n = N$ . It is easy to show that the value of  $c_N$  from Eq. (2) is for the limit of  $N \gg 1$ :

$$c_N = \omega_{\text{pl}} \lambda_j \frac{1}{\sqrt{1 + 2s - s[\pi/(N+1)]^2}}. \quad (3)$$

For the case of intrinsic stacks with a number of junctions  $N > 10$ , and  $s = 0.5$ , the lowest mode velocity  $c_N$  differs by less than 1% from its asymptotic value  $\omega_{\text{pl}} \lambda_j / \sqrt{2}$ .

In the flux-flow regime, the  $I$ - $V$  characteristic of a single long Josephson junction exhibits the flux-flow step. The voltage of the FFS is determined by the condition that the velocity of the moving fluxons reaches asymptotically the Swihart velocity. For a single long Josephson junction of length  $L$  with the magnetic thickness  $\Lambda = t + 2\lambda$ , the relation

$$U_{\text{FFS}} = \Phi_0 f = \bar{c} H \Lambda \quad (4)$$

holds, because  $H\Lambda L/\Phi_0$  gives the mean number of fluxons in the junction, and the frequency  $f$  is given by this number of fluxons divided by the time required for one fluxon at the Swihart velocity to pass through the junction. Note that the FFS voltage is directly proportional to the magnetic field  $H$ .

To investigate the flux-flow regime in stacked junctions, the system of coupled sine-Gordon equations (1) has been solved numerically via Fourier decomposition as described in Ref. 4. A set of  $I$ - $V$  characteristics for  $N = 11$ ,  $b = 20 \text{ \mu m}$ ,  $\beta_c = 20$ , and the BSCCO parameters from above is plotted in Fig. 1(a) for three external magnetic fields: 2.5, 4.5, and 6.5. Here the magnetic field is normalized to  $H_0 = \Phi_0/[b(t+d)\mu_0]$ , the field corresponding to one flux quantum per junction. We focus our interest on the part of the  $I$ - $V$  characteristic at low voltages. From the simulation, we see that in this regime, a triangular fluxon lattice of low density moves under the influence of the bias current. The resulting flux-flow branch in the  $I$ - $V$  characteristic is nearly linear for low current and turns up at higher current. For low magnetic fields, it ends by switching to the gap state at a

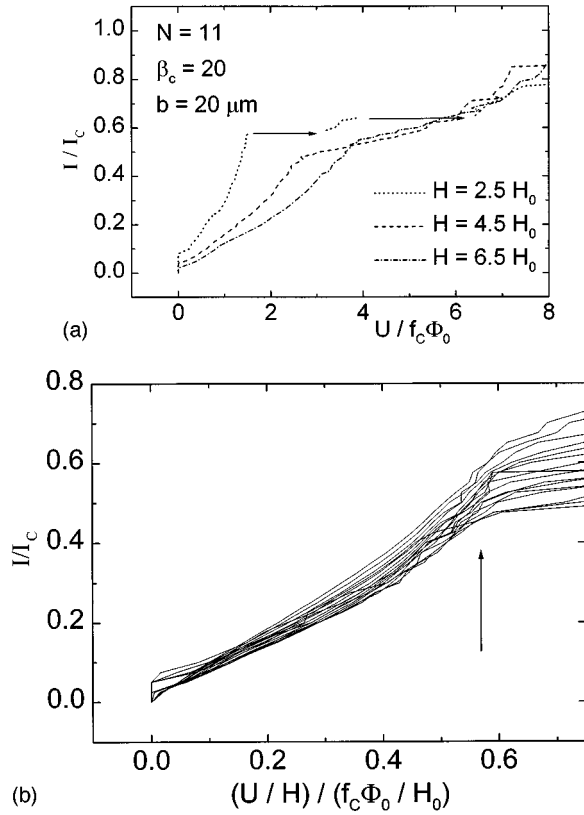


FIG. 1. (a) Superposition of numerically calculated  $I$ - $V$  characteristics of a stack of 11 Josephson junctions for three different magnetic fields.  $H_0 = \Phi_0 / [b(t+d)\mu_0]$  is the field corresponding to one flux quantum per junction. (b)  $I$ - $V$  characteristics for same parameters and fields from  $1.5$  to  $9.5 H_0$  in steps of  $0.5 H_0$ , plotted with voltage divided by field. Note that all curves show the kink at the same value for  $U/H$  as expected for a flux-flow step. For all simulations, values of  $\lambda_j = 1.1 \mu\text{m}$ ,  $\lambda_k = 1.5 \mu\text{m}$ ,  $b = 20 \mu\text{m}$ , and  $\beta_c = 20$  have been used.

certain field-dependent voltage. At higher fields, it kinks at this point and the voltage increases sharply but nonhysteretically. When all the  $I$ - $V$  curves for different field values are plotted with voltage divided by the magnetic field [Fig. 1(b)], it is obvious that this end of the flux-flow branch corresponds to the lowest collective-mode velocity  $c_N$ . The straightforward modification of the relation (4) for the first FFS in an intrinsic stack is

$$U_{\text{FFS}} = N\Phi_0 f = Nc_N H(t+d). \quad (5)$$

The factor of  $N$  appears because the stack is a series connection of junctions and the voltage will be measured over the whole stack. The factor  $(t+d)$  is the magnetic thickness of a junction with electrode thicknesses much less than  $\lambda$ . For the same parameters used in the numerical simulation Eq. (5) predicts the flux-flow step to appear at a normalized voltage  $U/H$  of  $0.590$  (in normalized units). This is in good agreement with the numerical result [see Fig. 1(b)], where all the flux-flow branches kink at  $U/H = 0.59$ .

### III. EXPERIMENT

#### A. Samples

Single crystals of BSCCO were grown in oxygen atmosphere by the floating-zone technique.<sup>13</sup> X-ray diffraction

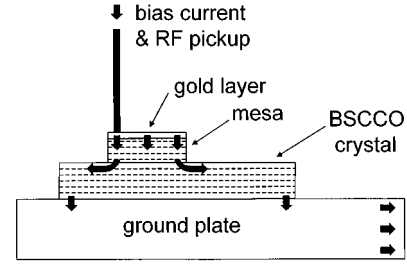


FIG. 2. Sketch of the sample geometry. Arrows indicate bias current flow. The gold layer on top of the mesa ensures homogeneous injection of bias current. The current leaves the mesa through the base crystal in a surface layer of thickness  $\lambda$  to a gold plated ground plate.

confirms that the crystals are single phase Bi-2212, and energy dispersive x-ray analysis indicates a cation stoichiometry of approximately Bi:Sr:Ca:Cu = 2.2:1.8:1.1:2. Using standard photolithography and Ar-ion etching, mesas of different lateral dimensions from  $20 \times 20 \mu\text{m}^2$  to  $40 \times 500 \mu\text{m}^2$  and of varying heights were fabricated on single-crystal surfaces. This technique provided stacks of about 30 to several hundreds of intrinsic Josephson junctions. On the top surface of the mesas, a low resistance gold layer was sputtered on the freshly cleaved  $a$ - $b$  faces. A sketch of the sample geometry showing the bias current flow is given in Fig. 2. A  $25 \mu\text{m}$  Au/Ni wire was used as a spring contact to the gold layer for applying bias current. In order to inject the bias current as homogeneous as possible, the gold layer extended over the whole top surface of the mesa. As the current leaves the mesa in a surface layer of thickness  $\lambda$  of the base crystal, as indicated in Fig. 2 by arrows, this configuration is quite close to the homogeneous current injection assumed in the numerical model. Due to the single top gold layer, a true four-point measurement of the  $I$ - $V$  characteristic was not possible, and the resulting contact resistance had to be subtracted for data evaluation. Several sample parameters are listed in Table I. Critical temperatures were around  $86 \text{ K}$ , critical current densities at  $4.2 \text{ K}$  were between  $500$  and  $600 \text{ A/cm}^2$ . Experiments on other high-frequency properties of intrinsic junctions not considering vortex motion are reported elsewhere.<sup>14</sup>

#### B. Setup

The magnetic field required for creating one flux quantum per junction in BSCCO is given by  $H_0 = \Phi_0 / [b(t+d)\mu_0]$ .

TABLE I. Dimensions, critical current densities, and critical temperatures of investigated samples.

Sample No.	Mesa size ( $\mu\text{m}^2$ )	Mesa height (nm)	$j_c$ ( $T=20 \text{ K}$ ) ( $\text{A/cm}^2$ )	$T_c$ (K)
D9b	$40 \times 40$	1200	580	85
D16a	$400 \times 20$	260	520	86
D16b	$200 \times 20$	260	520	86
D16c	$200 \times 10$	260	520	86
D16d	$500 \times 20$	260	520	86
D16e	$200 \times 5$	260	520	86

Here  $b$  is the length, and  $(t+d)=15 \text{ \AA}$  is the thickness of the junction. For a  $10 \text{ }\mu\text{m}$  long junction this equals to 1370 Oe. This field scale is not only two or three orders of magnitude larger than the fields required to create a flux quantum in artificially fabricated stacks but is also already larger than the lower critical field of the superconducting  $\text{CuO}_2$  layers (some tens of Oersteds). Thus, penetration of pancake vortices into the  $\text{CuO}_2$  layers is possible if the alignment of field and the crystals  $a$ - $b$  direction is not perfect. Because a stair-like vortex with pancakes has rather high pinning,<sup>15</sup> sample alignment is important for experiments on Josephson flux flow in BSCCO. To avoid the need of a cryogenic turnable broadband microwave connection that allows sample alignment in a standard magnet with vertical field, magnets with horizontal field were used. A horizontal magnetic field allows orientation of the sample by simply rotating the dipstick and a rigid microwave connection to the sample holder could be used. Either a superconducting 5 T split coil magnet or a pair of superconducting 1 T Helmholtz coils, both with horizontal field, were used.

Microwave signals were coupled out from the Au/Ni tip to a low loss coaxial cable and supplied to a low noise pre-amplifier for the frequency range from 6 to 18 GHz. The amplified signal was detected by a microwave spectrum analyzer. The overall noise temperature of this system was determined by hot/cold calibration and found to be approximately 550 K. Using this system in radiometer mode results in a sensitivity of  $3 \times 10^{-17} \text{ W}$  (30 aW) in a 3 MHz bandwidth with a typical integration time of 100 ms.

Sample bias current was provided by a battery powered current source to reduce external noise. Most measurements were performed in a shielded room.  $I$ - $V$  characteristics and microwave emission signals were recorded by digital voltmeters.

## IV. RESULTS AND DISCUSSION

### A. Influence of magnetic-field orientation

The  $I$ - $V$  characteristic of a stack of intrinsic Josephson junctions consists of many branches in zero magnetic field.<sup>6</sup> Below the critical current, due to the hysteresis, each junction can either be in its superconducting state or in the gap state. Thus each junction contributes one branch to the  $I$ - $V$  characteristic. For the experiments discussed here, the samples were biased in the state near zero voltage where no intrinsic junction has switched to its gap voltage.

To investigate the influence of misalignment between the magnetic field and the superconducting copper oxide layers, the sample was rotated at small angles around its position of perfect alignment, i.e., parallel to the layers. The sample was biased at a constant current corresponding to about 30–50 % of its zero-field critical current. The sample voltage was recorded as a function of angle for various fixed fields. The result is shown in Fig. 3 for one direction of angle sweep, to avoid hysteresis. For misorientation angles higher than some threshold angle  $\alpha_{\text{thr}}$ , the sample voltage is not influenced by the magnetic field and is equal to the voltage drop due to contact resistance. For angles smaller than the threshold angle, an additional voltage is present. As can be seen from the figure, this voltage increases with increasing field, whereas the threshold angle decreases. The perpendicular

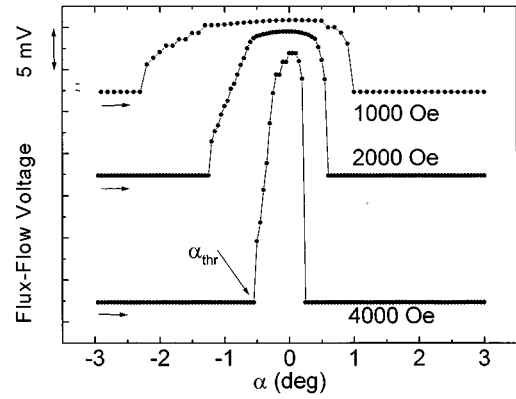


FIG. 3. Flux-flow voltage of No. D9b as a function of field misorientation angle  $\alpha$  at fixed bias current of 2.0 mA for three different fields. Temperature was 60 K. For clarity, the zero levels of the three curves are vertically shifted.

threshold field component  $H_{\text{thr}} = H \sin \alpha_{\text{thr}}$  is approximately constant for the different field values. Its value is around 30 Oe and of the same order of magnitude as the perpendicular  $H_{c1}$ . This behavior confirms that the observed voltage is caused by flux-flow of Josephson vortices. A flux-flow voltage will develop only for the case of vortex “lock-in”, because for higher angles of misorientation than  $\alpha_{\text{thr}}$ , pancake vortices are present in the superconducting layers, and the flux-line lattice will be pinned due to pinning of the pancakes.<sup>15</sup> This behavior was observed with all the samples investigated in this work, and was used routinely to adjust the parallel field orientation.

### B. $I$ - $V$ characteristics

For the state of parallel magnetic field,  $I$ - $V$  characteristics for various fields and temperatures were measured. With increasing field the former superconducting branch bends and exhibits a field-dependent flux-flow branch for low bias currents [Fig. 4(a)]. The slope  $R$  of this branch is proportional to the magnetic field and almost independent of temperature over a wide range of temperatures as can be seen from Fig. 4(b). We identify this branch with the displaced linear branch described in Ref. 9. In Fig. 5 we plot  $dR/dB$  vs the reciprocal mesa cross section for mesas with different lateral dimensions and the same height. As can be seen clearly, the slope of the linear branch scales with the inverse mesa area. This scaling shows that the flux-flow resistance only depends on the critical current, which is proportional to the mesa area. It is independent of the particular junction length. Whereas the observed branch is linear for low values of bias current it tends to turn up for higher bias currents. When a set of  $I$ - $V$  characteristics measured at different magnetic fields is plotted with the voltage divided by the field, the curves meet for high bias currents at some value of  $U/H$  (cf. Fig. 6). This behavior is quite similar to what we have found in our numerical simulations [cf. Fig. 1(b)]. There the observed branch was identified as a flux-flow step. The measured scaling behavior is also in agreement with Eq. (5), where  $U/H$  is determined only by the lowest collective-mode velocity. In particular, according to Eq. (5),  $U/H$  is independent of the junction length. This is also observed in the measurement.

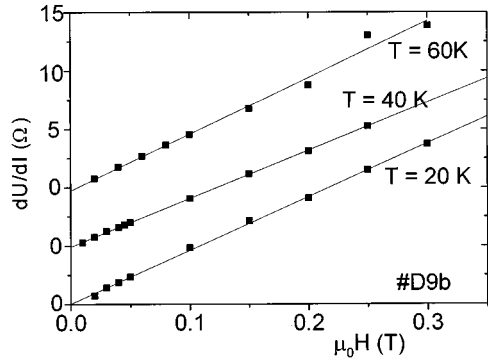
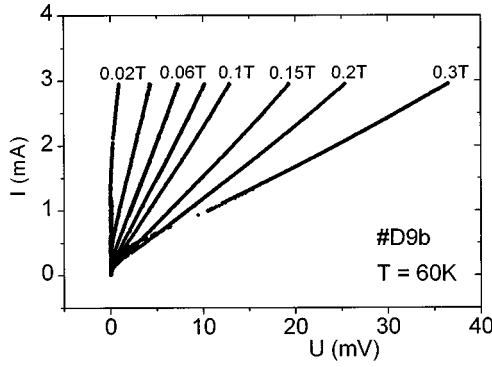


FIG. 4. (a)  $I$ - $V$  characteristic of linear displaced branch for eight values of magnetic field. (b) Field dependence of linear slope  $R = dU/dI$  for three different temperatures.

In contrast to the numerical simulation, in some measurements the curves normalized to  $U/H$  did not coincide perfectly at low bias currents. In particular, curves measured with large magnetic fields exhibited a somewhat smaller voltage. This behavior can be understood as follows: The flux-flow voltage of the whole stack is proportional to the number of Josephson junctions that take part in the flux flow. Due to defects, imperfect sample orientation or frozen pancake vortices, Josephson flux flow will be prevented in some

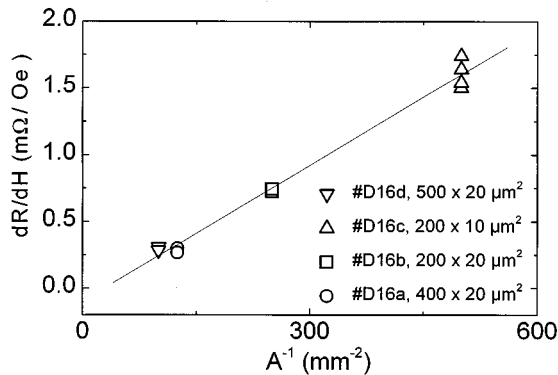


FIG. 5. Magnetic-field derivative of linear slope  $dR/dB$  vs the reciprocal mesa area ( $A^{-1}$ ) for mesas of different lateral dimensions and same height. Different data points for the same mesa correspond to measurements at different temperatures.

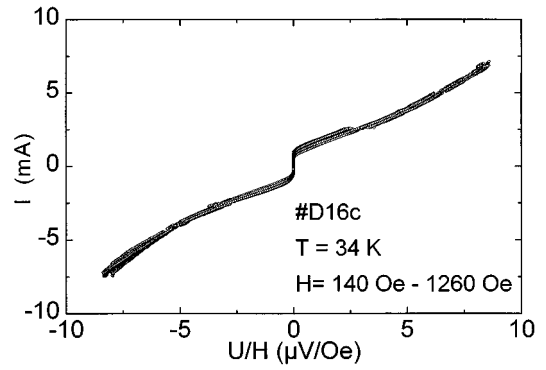


FIG. 6. Plot of  $I$ - $V$  characteristics for nine different values of magnetic field ranging from 140 to 1270 Oe with voltage divided by the magnetic field. Note that all curves collapse to one curve.

junctions by pinning. These junctions start to contribute to the fluxon motion only at higher bias current, when the Lorentz force on the vortices is high enough. In the case of slightly imperfect sample orientation, the density of pancake vortices increases with magnetic field and thus causes stronger pinning of the vortex lattice. It could be shown by the microwave emission data, that for a fixed field the number of junctions with flux flow is not constant, but increases with bias current (see below). To check if the observed deviation is influenced by pancake vortices, a set of  $I$ - $V$  characteristics was recorded for a sample intentionally misoriented by  $0.5^\circ$  from its optimum position. The deviation to lower voltages for low bias currents turned out to be stronger for the mis-oriented sample, whereas the flux-flow branch remained unchanged at higher bias currents.

The field-dependent slope of the  $I$ - $V$  curve was found to be nearly independent of temperature from 20 to 70 K, in spite of a strong variation of the characteristic voltage and the McCumber parameter over this temperature range. It is also known from observations of the displaced linear branch in single Josephson junctions, that its dependence on losses and thus temperature is very weak.<sup>16</sup>

The maximum value of  $U/H$ , corresponding to the lowest collective-mode velocity, was  $8.5 \mu\text{V/Oe}$  for the  $D16$  samples. Assuming a number of about 170 junctions in the stack (as expected from the measured mesa height), a value for the lowest collective-mode velocity of  $3.3 \times 10^5 \text{ m/s}$  can be derived. With an estimated Josephson penetration depth of  $0.5 \mu\text{m}$ , Eq. (3) yields a value of about 150 GHz for the plasma frequency. This value is in good agreement with data recently measured by microwave absorption measurements.<sup>17,18</sup>

### C. Microwave emission

Microwave emission measurements were carried out at various frequencies between 6 and 18 GHz. Depending on the receiver frequency, a broad emission peak showed up on the flux-flow branch of the  $I$ - $V$  characteristic. For coherent as well as for incoherent fluxon motion in a series connection of Josephson junctions the number of junctions contributing to the emission peak may be calculated by

$$N = \frac{U}{\Phi_0 f_{\text{rec}}}, \quad (6)$$

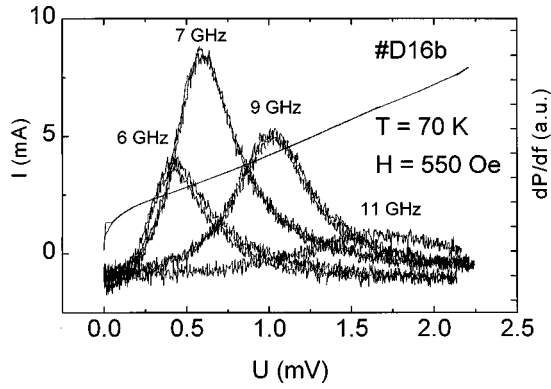


FIG. 7.  $I$ - $V$  characteristic (left scale) and microwave emission signal (right scale) for four detection frequencies at fixed magnetic field. With increasing receiver frequency, the peak shifts to higher voltages.

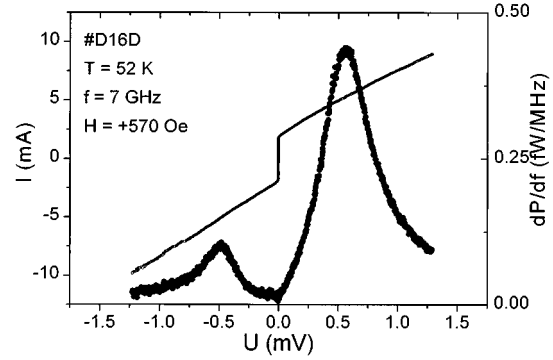
where  $U$  is the voltage at peak maximum and  $f_{\text{rec}}$  is the detected frequency. As shown in Fig. 7, the microwave emission peak shifts towards higher voltages when the receiver frequency is increased. However, the number of junctions derived from Eq. (6) also increases with frequency (or bias current): In the case of Fig. 7, the values for  $N$  for the frequencies 6, 7, 9, and 11 GHz are 34, 42, 55, and 73, respectively. This is consistent with the mesa height of 260 nm, giving a maximum of 170 junctions in the stack. We note that the observed increase of  $N$  with bias current counteracts the upturn of the flux-flow step. The upturn of this step would start at much lower bias currents if  $N$  were constant.

For the long mesas, the Au/Ni tip for bias current and microwave pick-up was attached to one end of the Josephson junction stack (see Fig. 2). For this geometry, the microwave signal intensity is expected to depend on the direction of fluxon motion.<sup>19</sup> As can be seen from Fig. 8, the detected microwave signal is asymmetric, and the intensity depends on the combination of bias current and magnetic-field polarities. When the magnetic field was reversed, the higher emission signal occurred at reversed bias current polarity. Note that reversing both magnetic field and bias current polarity results in the same direction of fluxon motion. The microwave signal was maximum for the case where the pickup tip is at that end of the stack where the vortices leave the junctions. This effect is well known for the flux-flow state in single long Josephson junctions.<sup>19</sup> Using Eq. (6), we find for the case of Fig. 8 that 40 intrinsic Josephson junctions are in the flux-flow regime.

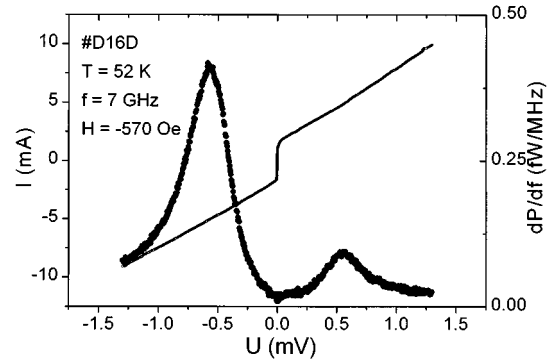
Using this value for the number of junctions, we find that the linewidth of the observed peak is about 6.3 GHz. For single fluxon radiation, the full linewidth at half power caused by pure Johnson-Nyquist noise is<sup>20</sup>

$$\Delta f = \frac{4\pi k_B T R_2^D}{\Phi_0^2 R_S}.$$

Here  $k_B$  is Boltzmann's constant,  $\Phi_0$  is the flux quantum,  $T$  is the temperature, and  $R_S$  and  $R_D$  are the resistance and differential resistance of the junction at the bias point. For our case this equals 17 MHz which is more than 300 times less than the experimental value. This enormous excess linewidth was typical for all our experiments. As described by



(a)



(b)

FIG. 8.  $I$ - $V$  characteristic and microwave emission signal for 500  $\mu\text{m}$  mesa for both polarities of the magnetic field. The microwave signal was coupled out at one end of the mesa. Note that the peak height corresponds to the *direction* of fluxon motion, i.e., the combination of magnetic field and bias current polarity. The high emission peak occurs when fluxons move towards the microwave pickup probe.

Golubov, Malomed, and Ustinov,<sup>21</sup> an excess linewidth in the flux-flow regime may be caused by internal degrees of freedom of the fluxon chain for a low density of vortices. Ustinov, Kohlstedt, and Henne observed a linewidth by a factor of  $10^4$  larger than the theoretical limit for the flux-flow state in a single long Josephson junction at low fluxon density.<sup>22</sup> As the fluxon lattice in a stack of Josephson junctions has even more degrees of freedom than the fluxon chain in a single junction—our fields correspond to a low vortex density—the same effect could be the reason for the observed huge excess linewidth in our case.

## V. CONCLUSIONS

We have investigated stacks of intrinsic Josephson junctions in BSCCO under the influence of a magnetic field parallel to the superconducting layers. From our measurements, as well as from comparison with simulations based on the coupled sine-Gordon equations for vertically stacked long Josephson junctions, we argue that the displaced linear branch observed in magnetic fields is associated with the flux-flow step caused by Josephson vortices moving collectively through many junctions of the stack. Their maximum velocity is close to the lowest collective-mode velocity of the

system. This is supported by a number of experimental observations. The observed amplitude of microwave emission signal is dependent on the direction of fluxon motion giving striking evidence that the displaced linear branch is a consequence of the motion of Josephson vortices. From the emission peak one infers that a large number of junctions in the stack contribute to radiation. For small values of bias current this number increases with increasing bias current. In a plot of current vs  $U/H$  all  $I$ - $V$  curves collapse at large values of bias current indicating that for large bias currents vortices move collectively in all junctions of the stack. Also, the enormous excess linewidth of the microwave emission signal is an indication that the observed flux flow is a regime where a triangular lattice of low fluxon density is moving through

the stack. In summary, all results show that the observed behavior can be understood as collective Josephson vortex motion in a stack of strongly coupled long Josephson junctions.

#### ACKNOWLEDGMENTS

We wish to thank D. Pooke for providing the BSCCO crystals, G. Kreiselmeier for setting up the 5 T magnet system, and A. V. Ustinov, L. N. Bulaevskii, and O. Waldmann for valuable discussions. Financial support by the Bayerische Forschungsförderung via the FORSUPRA consortium is gratefully acknowledged.

- 
- <sup>1</sup>N. F. Pedersen, *Physica D* **68**, 27 (1993).  
<sup>2</sup>R. D. Parmentier, in *The New Superconducting Electronics*, edited by H. Weinstock and R. Ralston (Kluwer, Dordrecht, 1993).  
<sup>3</sup>S. Sakai, P. Bodin, and N. F. Pedersen, *J. Appl. Phys.* **73**, 2411 (1993).  
<sup>4</sup>R. Kleiner, P. Müller, H. Kohlstedt, N. F. Pedersen, and S. Sakai, *Phys. Rev. B* **50**, 3942 (1994).  
<sup>5</sup>S. Sakai, A. V. Ustinov, H. Kohlstedt, A. Petraglia, and N. F. Pedersen, *Phys. Rev. B* **50**, 12 905 (1994).  
<sup>6</sup>R. Kleiner and P. Müller, *Phys. Rev. B* **49**, 1327 (1994).  
<sup>7</sup>F. Schmidl, A. Pfuch, H. Schneidewind, E. Heinz, L. Dörrer, A. Matthes, P. Seidel, U. Hübner, M. Veith, and E. Steinbeiss, *Supercond. Sci. Technol.* **8**, 740 (1995).  
<sup>8</sup>A. Yurgens, D. Winkler, N. V. Zavaritsky, and T. Claeson, *Phys. Rev. B* **53**, R8887 (1996).  
<sup>9</sup>J. U. Lee, J. E. Nordman, and G. Hohenwarter, *Appl. Phys. Lett.* **67**, 1471 (1995).  
<sup>10</sup>J. R. Clem and M. W. Coffey, *Phys. Rev. B* **42**, 6209 (1990).  
<sup>11</sup>L. N. Bulaevskii and J. R. Clem, *Phys. Rev. B* **44**, 10 234 (1991).  
<sup>12</sup>R. Kleiner, *Phys. Rev. B* **50**, 6919 (1994).  
<sup>13</sup>N. Motohira, K. Kuwahara, T. Hasegawa, K. Kishio, and K. Kitazawa, *J. Ceram. Soc. Jpn., Int. Ed.* **97**, 994 (1989).  
<sup>14</sup>G. Hechtfisher, K. Schlenga, W. Walkenhorst, P. Müller, A. Murk, W. Prusseit, M. Veith, W. Brodkorb, and E. Steinbeiss, *Microwave Properties of Intrinsic Josephson Junctions in High- $T_c$  Superconductors at Frequencies up to 95 GHz*, Proceedings of the 5th International Superconductive Electronics Conference (ISEC '95), Nagoya, Japan, 1995 (Institute of Physics Publishing, Bristol, 1996), p. 52.  
<sup>15</sup>L. N. Bulaevskii, M. Maley, H. Safar, and D. Dominguez, *Phys. Rev. B* **53**, 6634 (1996).  
<sup>16</sup>A. C. Scott and W. J. Johnson, *Appl. Phys. Lett.* **14**, 316 (1969).  
<sup>17</sup>Y. Matsuda, M. B. Gaifullin, K. Kumagai, K. Kadowaki, and T. Mochiku, *Phys. Rev. Lett.* **75**, 4512 (1995).  
<sup>18</sup>O. K. C. Tsui, N. P. Ong, and J. B. Peterson, *Phys. Rev. Lett.* **76**, 819 (1996).  
<sup>19</sup>T. Nagatsuma, K. Enpuku, K. Yoshida, and F. Irie, *J. Appl. Phys.* **56**, 3284 (1984).  
<sup>20</sup>E. Joergensen, V. P. Koshelets, R. Monaco, J. Mygind, M. R. Samuelsen, and M. Salerno, *Phys. Rev. Lett.* **49**, 1093 (1982).  
<sup>21</sup>A. A. Golubov, B. A. Malomed, and A. V. Ustinov, *Phys. Rev. B* **54**, 3047 (1996).  
<sup>22</sup>A. V. Ustinov, H. Kohlstedt, and P. Henne, *Phys. Rev. Lett.* **77**, 3617 (1996).